Atmos. Chem. Phys. Discuss., 14, 1051–1071, 2014
www.atmos-chem-phys-discuss.net/14/1051/2014/
doi:10.5194/acpd-14-1051-2014
© Author(s) 2014. CC Attribution 3.0 License.

Atmospheric Chemistry and Physics Discussions

This discussion paper is/has been under review for the journal Atmospheric Chemistry and Physics (ACP). Please refer to the corresponding final paper in ACP if available.

On transition-zone water clouds

E. Hirsch[1,2], I. Koren[1], Z. Levin[3,4], O. Altaratz[1], and E. Agassi[2]

[1]Department of Earth and Planetary Sciences, Weizmann Institute of Science, Rehovot 76100, Israel
[2]Department of Environmental Physics, Israel Institute for Biological Research, Nes-Ziona, Israel
[3]Department of Geophysical, Atmospheric and Planetary Sciences, Tel-Aviv University, Tel-Aviv, Israel
[4]The Energy, Environment and Water Research Center (EEWRC), The Cyprus Institute, Nicosia, Cyprus

Received: 26 November 2013 – Accepted: 5 January 2014 – Published: 13 January 2014

Correspondence to: I. Koren (ilan.koren@weizmann.ac.il)

Published by Copernicus Publications on behalf of the European Geosciences Union.

Abstract

A recent field campaign was conducted to measure the properties of thin, warm, convective clouds forming under conditions of weak updrafts. During the campaign, short-lived clouds (on the order of minutes) with droplets' effective radius of 1–2 µm and low liquid water path ($\sim 500\,\mathrm{mg\,m^{-2}}$) were measured. These low values are puzzling, since in most studies an effective radius of 4 µm is reported to serve as the lower bound for clouds. A theoretical cloud model designed to resolve the droplet-activation process suggested conditions that favor the formation of such clouds. Here we show that these clouds, which mark the transition from haze to cloud, are highly sensitive to the magnitude of the initial perturbation that initiated them. We define these clouds as "transition-zone clouds". The existence of such clouds poses a key challenge for the analysis of atmospheric observations and models, since they "further smooth" the transition from dry aerosol through haze pockets to cumulus clouds.

1 Introduction

Although extensively studied for decades, there is no clear definition of a cloud. Clouds are often defined by thresholds that depend on the measurement technique and application, such as the cloud optical depth (COD) threshold when using remote-sensing tools, or the liquid water content (LWC) threshold in cases of in-situ measurements and cloud numerical models. Such thresholds are not robust; they have been shown to misclassify the atmosphere and to introduce problems in analyses of both cloud and cloud-free regions (Koren et al., 2007; Charlson et al., 2007). On the micro-scale, the definition of a cloud droplet is more robust, since it is based on the clear physical discrimination between cloud and haze droplets, according to the Kohler theory (Kohler, 1936). A droplet that is large enough to grow spontaneously under environmental supersaturation is considered an activated cloud droplet. An inactivated droplet, which has not passed the thermodynamic barrier, is considered a haze droplet. Despite the

ACPD
14, 1051–1071, 2014

absence of a clear definition for clouds, there is general agreement that a substantial number of a cloud's droplets are activated. For example, continental subarctic low-level clouds have been found to contain an average fraction of activation of 47 % (with respect to number size distribution), with variations between 9 % and 86 % (Komppula et al., 2005).

There have been many studies on the temporal evolution of haze and cloud droplets (Mason and Chein, 1962; Mordy, 1959; Reutter et al., 2009). The presence of these two thermodynamic states, controlled by the degree of supersaturation, suggests an interesting evolution of the droplets' size-distribution function. Whereas haze is in a stable equilibrium, activated droplets are in an unstable equilibrium and their growth rate is inversely proportional to their radii. Such a diffusional growth rate dictates faster radial growth of small vs. bigger activated droplets. It has been shown that activated droplets in an ascending parcel reach a radius of more than 6 µm in less than 100 s, regardless of their initial size (Mordy, 1959). Therefore, the time during which the effective radius of the cloud droplet distribution is 1–3 µm is very short, and the likelihood of a cloud to obtain such an effective radius is very small. On the other hand, the differences in drop growth rates become negligible as they grow. The growth rate of activated droplets with radius larger than 10 µm depends mainly on the degree of supersaturation, rather than their size (Rogers, 1979). These properties create two droplet size gathering foci. One below the Kohler maxima that contains the haze particles, and the second one drifting toward the larger end of the spectrum of the growing activated droplets. Therefore, since the effective radius is biased toward the larger droplets, its value will usually be bigger than 1–3 µm. These considerations explain why a threshold radius of 4 µm is often used as the lowest value that can represent a cloud (Kawamoto et al., 2001), and why an effective radius in the range of 1–3 µm is considered transient, resulting in a small likelihood of capturing it for most cumulus clouds. These estimations agree well with observational records of effective radii of clouds. Extensive in-situ measurements (Miles et al., 2000) of global marine and continental low-level stratiform clouds gave a mean effective radius (r_{eff}) of 9.6 ± 2.35 µm and 5.4 ± 2.05 µm, respectively. In

ACPD
14, 1051–1071, 2014

addition, a nearly global survey of the effective radii in marine and continental shallow warm clouds (Han et al., 1994) indicated mean r_{eff} values of 11.8 µm and 8.5 µm, respectively. Nevertheless, small r_{eff} values, in the range of 3.5–5.5 µm, have been reported for in-situ measurements of continental boundary layer cumulus clouds (Han et al., 1995; Vogelmann et al., 2012). These values coincide well with the findings of Deng et al. (2009) who reported an average r_{eff} of 3.86 µm, with an average LWC of 0.16 g m^{-3}, from in-situ measurements of Cu clouds in Beijing. The smallest r_{eff} values were reported by Reid et al. (1999), who studied the properties of warm convective clouds in Brazil by in-situ measurements, and documented r_{eff} readings of 2 µm in a highly polluted environment. In addition, they provided a mathematical connection between the r_{eff} and the LWC which could explain 70 % of the variance in the measured data. Furthermore, in another study, a relationship between the liquid water path (LWP) and the r_{eff} of a cloud was found (Liu et al., 2003), suggesting that a small r_{eff} is positively correlated with small LWP.

During the eastern Mediterranean summer, it is typical to find stagnant atmospheric conditions, with a moist boundary layer and a near-neutral lapse rate that is bounded by an inversion layer. It was recently shown that small clouds forming under such conditions are characterized by a cloud base that is located a few hundred meters below the lifting condensation level (LCL) (Hirsch et al., 2013). In fact, in many cases, comparing the height of the LCL to the specific atmospheric profile predicted no cloud formation (LCL located above a strong inversion for example). It was suggested that these small clouds are the result of perturbations in relative humidity (RH) that drive parcel elevation at the mixing layer, rather than perturbations in temperature near the surface.

In this study, we focus on the very small end of the size distribution of convective clouds. During a recent field campaign (see next section for further details), we measured many short-lived Cu clouds (see an example in Fig. 1) that were characterized by very small r_{eff} values. Our study raises several questions: are these clouds? According to which definition can we identify them as clouds (remote sensing, modeling, micro-

ACPD
14, 1051–1071, 2014

physical)? Using theoretical cloud equations together with observations, we study the properties of this unique subset of clouds.

2 Methods

A field campaign was conducted during the summer (June–August) of 2011 in Israel, focusing on the microphysical and optical properties of thin, warm convective clouds. The cloud properties were retrieved using a novel ground-based hyperspectral technique (Hirsch et al., 2012) which was developed to retrieve the optical (COD) and microphysical (r_{eff}, LWP) properties of thin, warm clouds. The method was specifically designed to retrieve the properties of thin clouds and it relies on three elements: detailed radiative-transfer calculations in the longwave-IR regime, signal enhancement by subtraction of a clear sky reference, and a spectral matching method that exploits fine spectral differences between water droplets of different radii. The sensors were pointed to the zenith and the measurements were conducted at a rate of 0.5 Hz, thus the COD, r_{eff} and LWP were derived every 2 s.

The cloud-base height was measured by ceilometer at the Israeli Meteorological Service's (IMS) Beit-Dagan station, which is located approximately 10 km away from the cloud-measurement system. The IMS also measures atmospheric conditions twice a day by releasing a radiosonde from the Beit-Dagan station (at 0:00 UTC and 12:00 UTC). The data were downloaded from the University of Wyoming website (Website: atmospheric sounding). The radiosonde provides information on temperature, pressure, humidity, and horizontal wind speed profiles from the surface to the end of the troposphere. As explained later, the daily 12:00 UTC atmospheric profiles were used as input for the theoretical cloud model and to calculate the expected cloud-base height.

To examine the atmospheric conditions under which such clouds can form, a theoretical cloud model was developed. We used the basic cloud physics equations to investigate air-parcel evolution under weak updraft conditions, below a thermal inver-

ACPD
14, 1051–1071, 2014

sion (see Hirsch et al. (2013) for a comprehensive description of the parcel model). The droplet r_{eff} and supersaturation within the parcel, as well as the cloud's updraft and LWC were calculated for a range of initial conditions. The 24 dry aerosol size distributions used in the model were measured in situ in Europe and in the Mediterranean (Asmi et al., 2011), and the aerosols were assumed to be ammonium sulfate.

3 Results

Here we present a detailed case study of one day in the field campaign (30 June 2011, see the tephigram in Appendix A, Fig. A1). Analysis of the cloud measurements from that day revealed many short-lived clouds with uncommonly small r_{eff}. An example of one specific cloud is presented in Fig. 1. The cloud appears ordinary to the naked eye, and it has a short lifetime of only 6 min. Use of the retrieval method revealed the COD, LWP and r_{eff} as the cloud passed above the sensors in the zenith. The temporal average r_{eff} of the cloud (as it passed in the zenith) was 1.24 µm (with standard deviation of $\sigma = 0.2$ µm), the average LWP was 0.13 g m^{-2} ($\sigma = 0.14$ g m^{-2}), and the average COD at 550 nm was 9.15 ($\sigma = 11.3$). The data collected on this day showed many more clouds with similar characteristics. Most of the r_{eff} readings during noontime of that day were smaller than 2 µm (Fig. 2) and the clouds had a relatively short lifetime (several minutes at most).

Based on the sounding data from the Beit-Dagan meteorological station measured on 30 June 2011 at 12:00 UTC (15:00 LT), we simulated the formation of thin warm clouds on that day. A wide range of RH perturbations and initial vertical locations were used (presented in more detail further on). Figure 3 shows an example of one simulation of the formation of a small, warm cloud. To initiate the cloud formation we used a RH perturbation of 11 % above ambient RH (68 %), at a height of 550 m. The initial updraft of the parcel was set to zero, and its temperature was equal to the ambient temperature at that level (20.1 °C). Examination of Fig. 3 reveals that the parcel rose ∼ 475 m and reached a low supersaturation of ∼ 0.2 %, along with a LWC of

ACPD
14, 1051–1071, 2014

2.15 mg m^{-3}. The maximal r_{eff} of the droplets was 1.95 µm, while the parcel drifted up with a weak updraft (average of 86 cm s^{-1}), reaching a maximal value of 128 cm s^{-1} for a very short time (see Fig. 3). It is interesting to note the time lag between the maximal updraft and maximal LWC. At the stage of maximal updraft, the parcel contains only haze droplets, none of its droplets are activated and it is subvisual to the naked eye. When the parcel reaches its maximal LWC (and supersaturation), the updraft is completely exhausted, it turns into a downdraft and the cloud is already in the dissipation stage.

The dependency of the cloud's properties on the initial RH of the parcel was examined and the results are presented in Fig. 4. The ambient RH was 68 % and the perturbations ranged between 7 and 17 %. Every point in the figure represents the results of a complete simulation, similar to the one presented in Fig. 3. The maximal r_{eff} (blue), maximal RH (red), and maximal LWC (black) of the forming clouds were plotted against the initial RH of the parcel. To emphasize the dependency of the maximal r_{eff} on initial RH, we plotted the derivative of the blue line ($r_{eff,\,max}$) against RH_{init} ($d(r_{eff,\,max})/d(RH_{init})$, in green). We defined the cases with $d(r_{eff,\,max})/d(RH_{init})$ > 2 µm %$^{-1}$ as "transition-zone" clouds (marked with vertical magenta lines). The clear and narrow transition zone seen in all of the graphs (r_{eff}, RH and LWC) implies that these clouds are highly sensitive to the initial conditions of the parcel. Furthermore, it reinforces the common assumption of a minimal r_{eff} of 4 µm for clouds, located well beyond the transition zone.

Although the marked region appears small, it does not necessarily represent the likelihood of such conditions in nature; in fact, it represents a wide range of possible values. The range of the maximal r_{eff} is from 0.43 to 2.67 µm, while the range of the maximal LWC is between 0.1 and 14.1 mg m^{-3}. In addition, maximal supersaturation ranges between 0.07 and 0.31 %, whereas the average updraft is approximately constant at 0.86 m s^{-1}. Furthermore, it is possible to define a criterion for the cloud's lifetime. For every simulated cloud, we defined its lifetime as the period during which

ACPD
14, 1051–1071, 2014

the r_{eff} exceeds 0.5 µm. Using this definition, the range of possible lifetimes spans up to 1.4 min.

Further examination of the model results for a range of different initial vertical locations of the parcel and initial RH values, revealed a range of possible values for the microphysical properties and lifetimes of the formed clouds. In every panel in Fig. 5, the temperature (blue) and RH (red) profiles are plotted along with the ceilometer measurement of cloud-base height (horizontal blue line) and the theoretical LCLs (horizontal cyan and magenta lines). One of the LCL calculations was based on a ground-level ascending parcel and the other on a parcel with average properties of the lowest 500 m. First, we note that the measured cloud base is ∼ 500 m below the LCL. This phenomenon has been reported by Hirsch et al. (2013), and it suggests that such clouds must be a result of RH perturbations in the mixing layer. Figure 5a supports this hypothesis: the lower symbol of every pair of symbols represents both the initial height of the parcel and the size of the smallest RH perturbation that created a cloud (determined by a threshold of RH > 100 %). The higher symbol of every pair represents the simulated cloud-base height. The figure presents only cases which resulted in cloud-base heights similar to the measured height (initial heights between 250 and 750 m). Figure 5b–f presents the possible values of maximal r_{eff}, maximal LWC, maximal supersaturation, lifetime, and average updraft, respectively. The colored region corresponds to the value of the simulated parameter. The position of the colored region on the graph represents the initial height of the parcel and the magnitude of the RH perturbation.

By analyzing the results presented in Fig. 5 and following the definition of transition-zone clouds, it is possible to calculate the possible supersaturation, LWC and r_{eff} values of those clouds, while considering different heights from which the parcel might have started to ascend. The maximal r_{eff} varies between 0.41 and 2.69 µm, while the maximal LWC ranges between 0.09 and 16.8 $mg\,m^{-3}$. The maximal supersaturation varies between 0.05 and 0.33 % and the average updraft ranges between 0.62 and 1.15 $m\,s^{-1}$. When considering the possible initial heights of the parcel, the lifetime of the transition-zone clouds may reach 13.5 min, but it is often much shorter.

ACPD
14, 1051–1071, 2014

How sensitive are these results to the aerosol model? To study the effect of dry aerosol size distribution on the properties of the forming clouds, we used 24 types of dry aerosol size distributions that had been measured in situ in Europe and the Mediterranean region (Asmi et al., 2011). Figure 6 demonstrates that the phenomenon of transition-zone clouds is independent of the dry aerosol size distribution, although the microphysical properties (LWC, supersaturation, r_{eff}) of the forming clouds are affected. Fig. 6 presents a group of curves representing the results of 3.192 different simulations for 24 types of dry aerosol size distributions (every distribution with 133 different initial RH perturbations). The maximal r_{eff} of the droplets is presented vs. the maximal LWC in the cloud. All parcels were initiated at a height of 550 m, while every point on the curves represents a full simulation, similar to the one presented in Fig. 3, for a different initial dry aerosol size distribution and different initial RH perturbation. An examination of the curves shows the regime in this phase space, dominated by "transition-zone" clouds. This regime is determined based on the presented criterion for recognizing the zone of sharp change in cloud properties as a function of the initial RH perturbation for similar dry aerosol distribution simulations (see explanation of Fig. 4). In a subsaturated air parcel, haze develops with a submicron r_{eff} (shaded yellow region). On the other hand, initial perturbation with relatively high RH compared to the environment (shaded blue region) can produce more developed clouds that are characterized by larger r_{eff} and higher LWC. In the intermediate zone (shaded magenta region), transition-zone clouds are formed, namely clouds that are transitional between haze and Cu clouds. They are, by definition, highly sensitive to the initial RH perturbation. When considering the wide range of possible dry aerosol size distributions, the maximal r_{eff} may vary between 1.5 and 6 µm, while the maximal LWC ranges between 0.01 and 73 $\mathrm{mg\,m^{-3}}$. The supersaturation can be as high as 0.6 %, while the average updraft is almost unaffected by the aerosol size distribution (range of 0.85–0.87 $\mathrm{m\,s^{-1}}$).

Obviously, the occurrence of transition-zone clouds is not restricted to the eastern Mediterranean region. Similar atmospheric conditions are quite common during the summer in other locations around the globe (specifically coastal areas along the sub-

ACPD
14, 1051–1071, 2014

tropical belt, see Fig. 7 and discussion in Hirsch et al., 2013), in which a persistent synoptic-scale subsidence exists. In such places, it is common to see small (on the scale of 100 m) cumulus clouds that form and dissipate within a few minutes.

4 Summary and discussion

In this study, we focused on a cloud regime that is usually overlooked. Observational evidence for warm clouds with small r_{eff}, small LWP, and a short lifetime were found during a field campaign. These observations initiated a detailed analysis using a bin microphysics cloud model to study the microphysical properties of small, short-lived convective clouds that form as a result of RH perturbations which can drive weak updrafts in a humid boundary layer bounded by a thermal inversion. The model predicts that under such conditions, a special subset of clouds with unique microphysical properties can form. Such clouds are defined here as transition-zone clouds because their thermodynamic state is in the transition between haze and cumulus clouds. They are highly sensitive to the initial perturbation, and they are characterized by a $r_{\mathrm{eff}} <\sim 3\,\mu\mathrm{m}$, which is conventionally considered below the threshold of cumulus clouds. Such clouds contain a relatively low LWC ($< 17\,\mathrm{mg\,m^{-3}}$), and have a small COD. In addition, these clouds reach their maximal LWC when their driving updraft has already dissipated.

Because of their temporal and spatial properties, such clouds are likely to escape the scientific "cloud radar". Small, short-lived clouds form a collective suite of challenges to study. Their physical properties fall below most of the sampling rate and sensitivity limits of in-situ measurement instruments, and are smaller than the spatial resolution of most climate-oriented remote sensing sensors. Moreover, most of the RH measurement techniques are limited to a lower supersaturation bound of 0.2 % (Snider et al., 2003); and measurements of low supersaturation are difficult to perform and are usually highly inaccurate (Rose et al., 2008). It is therefore quite hard to characterize these clouds.

ACPD
14, 1051–1071, 2014

This study raises several interesting and important issues regarding the way in which clouds are defined. Our results can be generalized, suggesting that many of the convective clouds whose maximal size is in the range of a few hundred meters or less, and that form below an inversion layer, are likely to be the result of a weak perturbation located not far below the inversion base height. Such perturbations lift the parcel, developing low supersaturation and creating clouds.

It has already been noted that the region between clouds within a cloud field (also known as the clouds' twilight zone; Koren et al., 2007) is characterized by unique optical properties, and that the commonly used discrimination between clear and cloudy skies might lead to substantial errors in estimating radiative forcing (Charlson et al., 2007). In this paper, we explore the range of small clouds that lie between haze and conventional, more developed cumulus clouds, and introduce the transition-zone cloud. Although these clouds seem to exist for only a relatively small range of initial conditions, they are expected to be quite common, since they form in common environmental conditions. Moreover, a link is expected between the clouds' size and frequency of occurrence (Koren et al., 2008; Wood and Field, 2011; Zhao and Girolamo, 2007). As these clouds occupy the small end of the Cu cloud size distribution, their number is the highest. These findings suggest that the subset of transition-zone clouds has an important radiative forcing effect which is currently either not considered, or wrongly attributed to aerosols.

Furthermore, these clouds might better explain the unique optical properties of the clouds' twilight zone. Our findings suggest that weight should be given to theoretical studies, as well as to the development of instruments and measuring techniques that will enable us to advance our knowledge of this important and understudied subset of clouds.

ACPD
14, 1051–1071, 2014

Appendix A

The atmospheric profile used in this study

See Fig. A1.

Acknowledgements. The research leading to these results was funded by the European Research Council under the European Union's Seventh Framework Programme (FP7/2007–2013)/ERC Grant agreement no. [306 965].

References

Asmi, A., Wiedensohler, A., Laj, P., Fjaeraa, A.-M., Sellegri, K., Birmili, W., Weingartner, E., Baltensperger, U., Zdimal, V., Zikova, N., Putaud, J.-P., Marinoni, A., Tunved, P., Hansson, H.-C., Fiebig, M., Kivekäs, N., Lihavainen, H., Asmi, E., Ulevicius, V., Aalto, P. P., Swietlicki, E., Kristensson, A., Mihalopoulos, N., Kalivitis, N., Kalapov, I., Kiss, G., de Leeuw, G., Henzing, B., Harrison, R. M., Beddows, D., O'Dowd, C., Jennings, S. G., Flentje, H., Weinhold, K., Meinhardt, F., Ries, L., and Kulmala, M.: Number size distributions and seasonality of submicron particles in Europe 2008–2009, Atmos. Chem. Phys., 11, 5505–5538, doi:10.5194/acp-11-5505-2011, 2011.

Atmospheric sounding: available at: http://weather.uwyo.edu/upperair/sounding.html, last access: October 2013.

Charlson, R. J., Ackerman, A. S., Bender, F. A. M., Anderson, T. L., and Liu, Z.: On the climate forcing consequences of the albedo continuum between cloudy and clear air, Tellus B, 59, 715–727, 2007.

Deng, Z., Zhao, C., Zhang, Q., Huang, M., and Ma, X.: Statistical analysis of microphysical properties and the parameterization of effective radius of warm clouds in Beijing area, Atmos. Res., 93, 888–896, 2009.

Han, Q., Rossow, W. B., and Lacis, A. A.: Near-global survey of effective droplet radii in liquid water clouds using ISCCP data, J. Climate, 7, 465–497, 1994.

Han, Q., Welch, R., Chou, J., Rossow, W., and White, A.: Validation of satellite retrievals of cloud microphysics and liquid water path using observations from FIRE, J. Atmos. Sci., 52, 4183–4195, 1995.

ACPD
14, 1051–1071, 2014

Hirsch, E., Agassi, E., and Koren, I.: Determination of optical and microphysical properties of thin warm clouds using ground based hyper-spectral analysis, Atmos. Meas. Tech., 5, 851–871, doi:10.5194/amt-5-851-2012, 2012.

Hirsch, E., Koren, I., Altaratz, O., Levin, Z., and Agassi, E.: Perturbations in relative humidity in the boundary layer represent a possible mechanism for the formation of small convective clouds, Atmos. Chem. Phys. Discuss., 13, 28729–28749, doi:10.5194/acpd-13-28729-2013, 2013.

Kawamoto, K., Nakajima, T., and Nakajima, T. Y.: A global determination of cloud microphysics with AVHRR remote sensing, J. Climate, 14, 2054–2068, 2001.

Köhler, H.: The nucleus in and the growth of hygroscopic droplets, T. Faraday Soc., 32, 1152–1161, 1936.

Komppula, M., Lihavainen, H., Kerminen, V. M., Kulmala, M., and Viisanen, Y.: Measurements of cloud droplet activation of aerosol particles at a clean subarctic background site, J. Geophys. Res.-Atmos., 110, D06204, doi:10.1029/2004JD005200, 2005.

Koren, I., Remer, L. A., Kaufman, Y. J., Rudich, Y., and Martins, J. V.: On the twilight zone between clouds and aerosols, Geophys. Res. Lett., 34, L08805, doi:10.1029/2007GL029253, 2007.

Koren, I., Oreopoulos, L., Feingold, G., Remer, L. A., and Altaratz, O.: How small is a small cloud?, Atmos. Chem. Phys., 8, 3855–3864, doi:10.5194/acp-8-3855-2008, 2008.

Liu, G., Shao, H., Coakley, J. A., Curry, J. A., Haggerty, J. A., and Tschudi, M. A.: Retrieval of cloud droplet size from visible and microwave radiometric measurements during INDOEX: implication to aerosols' indirect radiative effect, J. Geophys. Res.-Atmos., 108, 4006, doi:10.1029/2001JD001395, 2003.

Mason, B. and Chien, C.: Cloud-droplet growth by condensation in cumulus, Q. J. Roy. Meteor. Soc., 88, 136–142, 1962.

Miles, N. L., Verlinde, J., and Clothiaux, E. E.: Cloud droplet size distributions in low-level stratiform clouds, J. Atmos. Sci., 57, 295–311, 2000.

Mordy, W.: Computations of the growth by condensation of a population of cloud droplets, Tellus, 11, 16–44, 1959.

Reid, J. S., Hobbs, P. V., Rangno, A. L., and Hegg, D. A.: Relationships between cloud droplet effective radius, liquid water content, and droplet concentration for warm clouds in Brazil embedded in biomass smoke, J. Geophys. Res.-Atmos., 104, 6145–6153, 1999.

ACPD
14, 1051–1071, 2014

Reutter, P., Su, H., Trentmann, J., Simmel, M., Rose, D., Gunthe, S. S., Wernli, H., Andreae, M. O., and Pöschl, U.: Aerosol- and updraft-limited regimes of cloud droplet formation: influence of particle number, size and hygroscopicity on the activation of cloud condensation nuclei (CCN), Atmos. Chem. Phys., 9, 7067–7080, doi:10.5194/acp-9-7067-2009, 2009.

Rogers, R.: A Short Course in Cloud Physics, Pergamon Press, International Series in Natural Philosophy, 96, Oxford and Elmsford, N. Y., 246, 1979.

Rose, D., Gunthe, S. S., Mikhailov, E., Frank, G. P., Dusek, U., Andreae, M. O., and Pöschl, U.: Calibration and measurement uncertainties of a continuous-flow cloud condensation nuclei counter (DMT-CCNC): CCN activation of ammonium sulfate and sodium chloride aerosol particles in theory and experiment, Atmos. Chem. Phys., 8, 1153–1179, doi:10.5194/acp-8-1153-2008, 2008.

Snider, J. R., Guibert, S., Brenguier, J. L., and Putaud, J. P.: Aerosol activation in marine stratocumulus clouds: 2. Köhler and parcel theory closure studies, J. Geophys. Res.-Atmos., 108, 8629, doi:10.1029/2002JD002692, 2003.

Vogelmann, A. M., McFarquhar, G. M., Ogren, J. A., Turner, D. D., Comstock, J. M., Feingold, G., Long, C. N., Jonsson, H. H., Bucholtz, A., and Collins, D. R.: RACORO extended-term aircraft observations of boundary layer clouds, B. Am. Meteorol. Soc., 93, 861–878, 2012.

Wood, R. and Field, P. R.: The distribution of cloud horizontal sizes, J. Climate, 24, 4800–4816, 2011.

Zhao, G. and Di Girolamo, L.: Statistics on the macrophysical properties of trade wind cumuli over the tropical western Atlantic, J. Geophys. Res.-Atmos., 112, D10204, doi:10.1029/2006JD007371, 2007.

ACPD
14, 1051–1071, 2014

Fig. 1. Images taken during a field campaign on 30 June 2011 at 15:52–15:56 LT. Top: sequential (1 min time lag) images of the complete lifetime of a single short-lived cloud. The camera was pointed at the zenith and the diagonal field of view is 180°. The yellow rectangles mark the position of the cloud. Bottom: enlargement of one of the images.

ACPD
14, 1051–1071, 2014

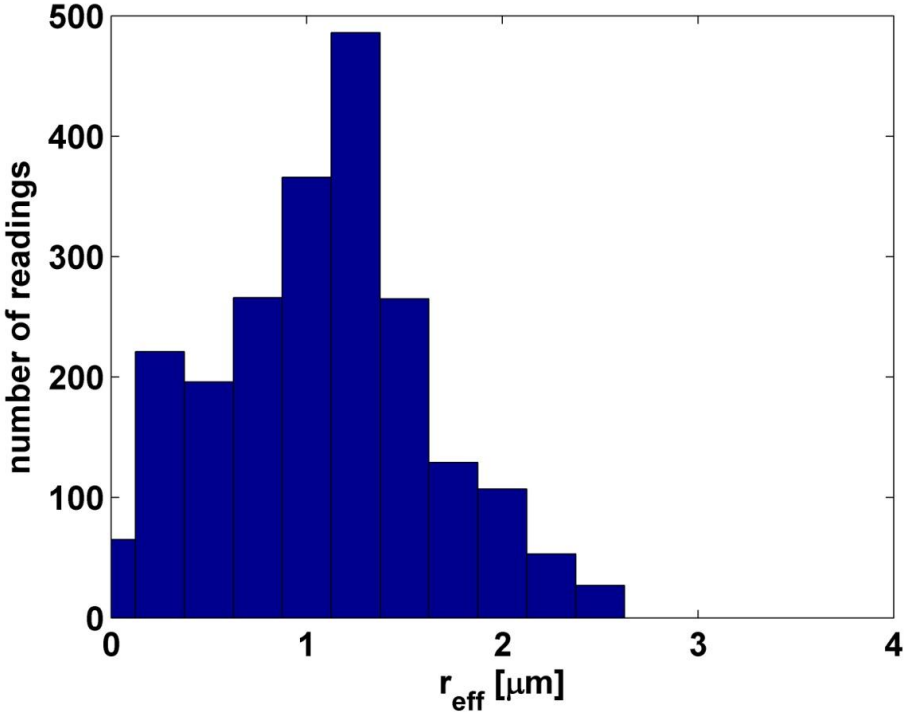

Fig. 2. A histogram of effective radius (r_{eff}) readings from 14:00–16:00 LT on 30 June 2011. Most of the r_{eff} readings are below 2 µm. Data were measured at a rate of 0.5 Hz.

ACPD
14, 1051–1071, 2014

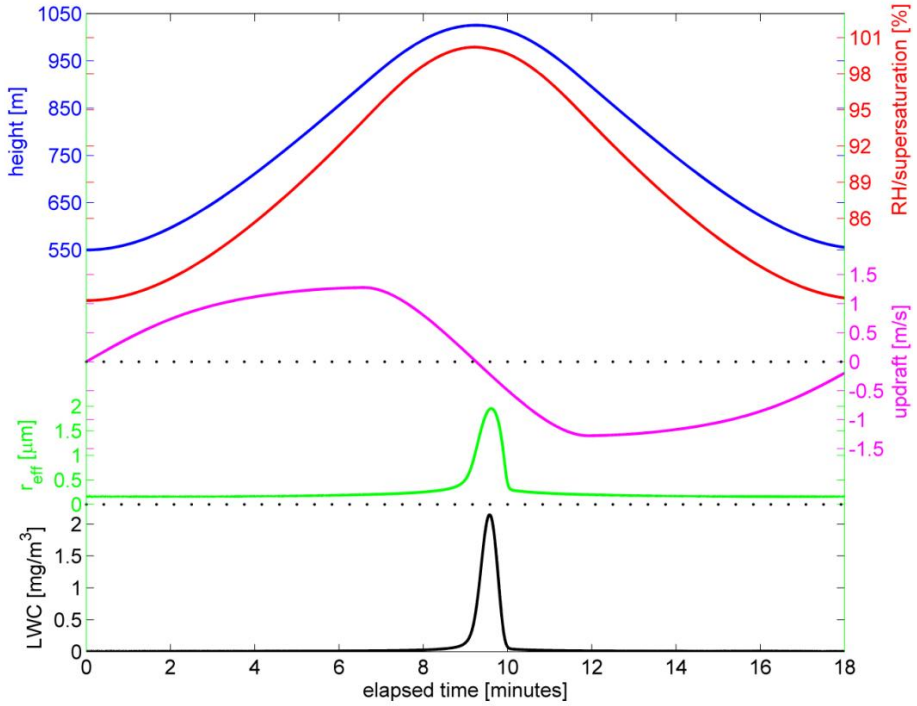

Fig. 3. Temporal evolution of an air parcel. Vertical position (blue), relative humidity (RH) and supersaturation (red), updraft (magenta), effective radius (r_{eff}, green), and liquid water content (LWC, black).

ACPD
14, 1051–1071, 2014

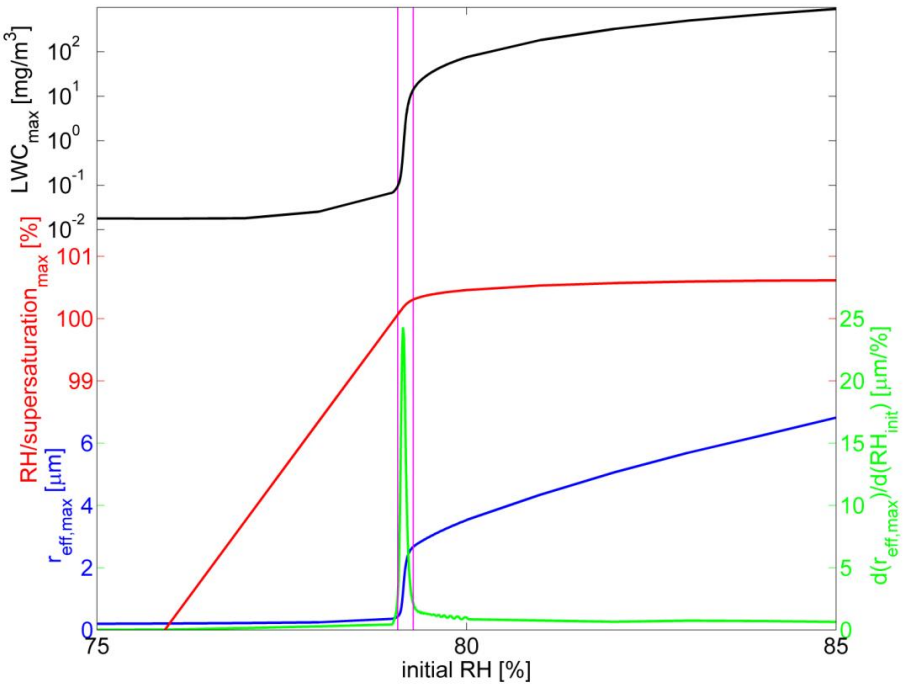

Fig. 4. The maximal effective radius (r_{eff}, blue), maximal relative humidity (RH, red), and maximal liquid water content (LWC, black) of the forming clouds vs. the initial RH of the parcel. The green line is the derivative of the maximal r_{eff} with respect to the initial RH of the parcel. Transition-zone clouds are defined within the vertical magenta lines (see text for further explanation).

ACPD
14, 1051–1071, 2014

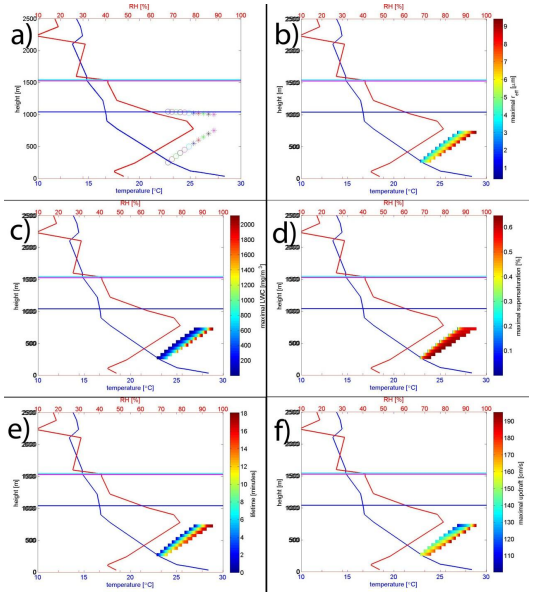

Fig. 5. Theoretical cloud model results for a range of possible initial heights and relative humidity (RH) perturbations for the atmospheric profile of 30 June 2011, 12:00 UTC. **(a)** The lower symbol of every pair of symbols represents both the initial height of the parcel and the size of the smallest RH perturbation that created a cloud (determined as RH > 100 %). The higher symbol of every pair represents the simulated cloud-base height. Note that all of the simulated parcels (initial heights 250–750 m) resulted in a cloud base at the measured value (horizontal blue line). **(b)** Possible values of the maximal effective radius (r_{eff}) for different initial heights and different perturbations. The colored region corresponds to the value of the simulated maximal r_{eff}. The position of the colored region on the graph represents the initial height of the parcel and the magnitude of the RH perturbation. **(c–f)** Same as panel **(b)** but for maximal liquid water content (LWC), maximal supersaturation, lifetime, and average updraft, respectively.

ACPD
14, 1051–1071, 2014

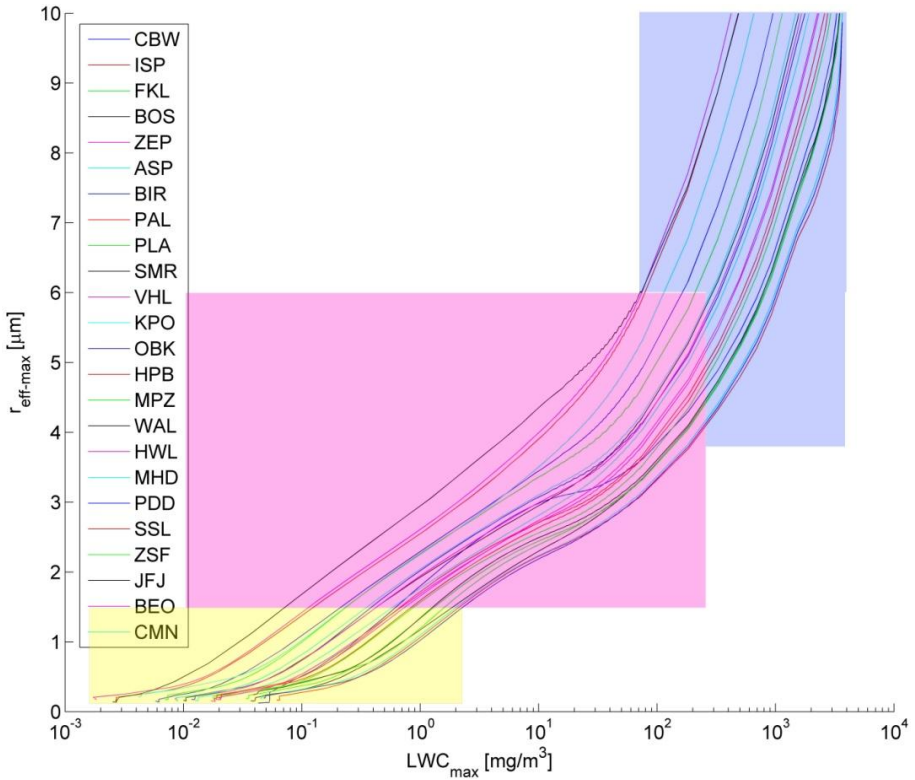

Fig. 6. The maximal effective radius ($r_{eff\text{-}max}$) vs. the maximal liquid water content (LWC_{max}) in the cloud for different dry aerosol size distributions (Asmi et al., 2011) and different initial relative humidity perturbations. Each line represents a different dry aerosol size distribution. The labels follow the names given by Asmi et al. (2011). The different shaded regions represent conditions of haze (subsaturation, yellow), transition-zone clouds (magenta), and more developed Cu clouds (blue).

ACPD
14, 1051–1071, 2014

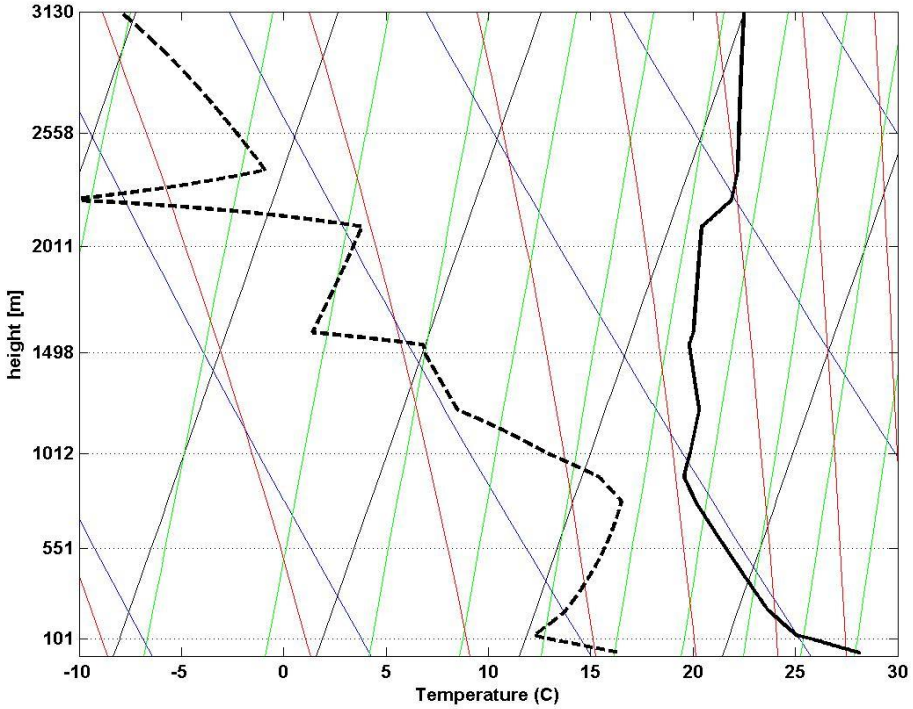

Fig. A1. Tephigram of the atmospheric profile used in the model.

ACPD
14, 1051–1071, 2014